Ultrasonic Studies of the Superconductivity of Doped Tin

LEWIS T. CLAIBORNE AND NORMAN G. EINSPRUCH
Texas Instruments Incorporated, Dallas, Texas
(Received 22 June 1966)

Detailed information concerning the anisotropy of the effective limiting superconducting energy gap $\Delta(0)$ of doped Sn has been obtained from measurements of the temperature dependence of the attenuation of compressional ultrasonic waves. Earlier results for the In-doped Sn system have been confirmed for other impurities, and analysis of the results has been made in terms of recent developments in the theory of dirty superconductivity. Measurements have been made for the sound-propagation vector $\mathbf{q}$ parallel to the [001], [110], and [100] directions in single crystals of In-, Cd-, Sb-, and Bi-doped Sn with impurity concentrations ranging from ~1 to 5 000 parts per million (ppm). The measured anisotropy between the [110] and [001] directions for pure Sn is ~20% of the average energy gap. It is found that this anisotropy is reduced to ~2% for values of the inverse resistivity ratio $\rho \gtrsim 10^{-2}$ and for $\Delta T_c > 15$ mdegK. BCS theory, which was developed for isotropic, weak-coupling superconductors, is applicable to the most heavily doped samples; it is found that the energy gap ($\sim 1.76 k_B T_c$) and the temperature dependence of ultrasonic attenuation are in agreement with the predictions of the theory. By comparing the energy-gap measurements from tunneling data with the energy gap obtained from ultrasonic-attenuation data, it is possible to demonstrate that the temperature dependence of the attenuation gives a measure of more than one energy gap. In addition to the gap obtained from the attenuation data at low temperatures, a larger gap can be observed near T_c. From tunneling data, the larger gap for $\mathbf{q} \| [001]$ is $(1.9 \pm 0.05) k_B T_c$; the ultrasonic determination yields $(1.92 \pm 0.02) k_B T_c$. In addition, the temperature dependence of the larger gap is obtained near T_c and is compared with BCS theory. For $[1 - T/T_c]$ ranging from $\sim 4 \times 10^{-2}$ to $\sim 4 \times 10^{-1}$, it is found that the BCS-predicted approximation, $\Delta(T)/\Delta(0) = 1.74[1 - T/T_c]^{1/2}$, is accurate to ~2%.

THE detailed relationships between the anisotropy of the superconducting energy gap and the electronic band structure, the phonon density of states, and the impurity concentration are among the important problems remaining in the field of type-I superconductivity.[1] Studies of the temperature dependence of ultrasonic attenuation in many superconductors have yielded much information about energy-gap anisotropy.[2] The present work is concerned with a study of the influence of impurities on the anisotropy and with extending further the procedure for extracting information from the ultrasonic measurements. Since the most detailed energy-gap measurements are those that have been made on Sn, both by the ultrasonic[2–4] and the electron-tunneling[5] techniques, the Sn system was chosen for this study. The temperature dependence of the compressional-wave attenuation at frequencies from 30 to 460 MHz was measured in the [001], [110], and [100] directions in a variety of In-, Sb-, Bi-, and Cd-doped Sn single crystals with impurity concentrations ranging from ~1 to ~5000 parts per million. The data have been analyzed in terms of the several existing models for the attenuation in anisotropic superconductors. The theoretical motivation for the measurements and an improved experimental technique are discussed in Secs. I and II. In Secs. III and IV a detailed comparison is made between the tunneling data and the effective energy gap obtained from the ultrasonic data. An attempt is made to determine the meaning of the limiting energy gap estimated in previous studies. Finally, the variation of the transition temperature with impurity concentration in the single crystals is compared with polycrystalline data and with the existing theory of dirty superconductors.

I. THEORETICAL BACKGROUND

Before considering the ultrasonic attenuation in a complicated metal such as Sn, it is necessary to recall the results obtained in the free-electron limit for an isotropic material with a well defined relaxation time τ. Pippard[6] has shown that in this approximation the compressional-wave attenuation due to the interaction between the crystal lattice and the conduction electrons is

$$\alpha_n = \frac{N m_e}{\rho_0 C_s \tau}\left[\frac{(q l_e)^2 \tan^{-1} q l_e}{3(q l_e - \tan^{-1} q l_e)} - 1\right]. \quad (1)$$

(All symbols are defined in the glossary below.) The normal-state attenuation is a monotonic increasing function of $q l_e$. In general, $q l_e \gtrsim 1$ for the electronic attenuation to be sufficiently large to be readily measurable. BCS[7] theory predicts that for an isotropic superconductor the ratio of the compressional-wave attenuation in the superconducting state to that in the normal state is given by

$$\alpha_s/\alpha_n = 2f[\epsilon_0(T)] = 2\{\exp[\epsilon_0(T)/k_B T] + 1\}^{-1}, \quad (2)$$

[1] D. H. Douglass, Jr., and L. M. Falicov, in *Progress in Low Temperature Physics*, edited by C. J. Gorter (North-Holland Publishing Company, Amsterdam, 1964), Vol. IV, pp. 97–193.
[2] R. W. Morse, T. Olsen, and J. D. Gavenda, Phys. Rev. Letters **3**, 15 (1959).
[3] J. R. Leibowitz, Phys. Rev. **133**, A84 (1964).
[4] P. A. Bezuglyi, A. A. Galkin, and A. P. Korolyuk, Zh. Eksperim. i Teor. Fiz. **39**, 7 (1960) [English transl.: Soviet Phys.—JETP **12**, 4 (1960)].
[5] N. V. Zavaritskii, Zh. Eksperim. i Teor. Fiz. **48**, 837 (1965) [English transl.: Soviet Phys.—JETP **21**, 557 (1965)].
[6] A. B. Pippard, Phil. Mag. **46**, 1104 (1955).
[7] J. Bardeen, L. N. Cooper, and J. R. Schrieffer, Phys. Rev. **108**, 1175 (1957).

where $\epsilon_0(T)$ is the *isotropic* temperature-dependent superconducting energy gap. This result has been shown to be independent of sound frequency and electron mean free path for impurity-limited scattering.[8] Morse *et al.*[2] and Leibowitz[3] have assumed that the form of Eq. (2) is correct for anisotropic superconductors, but that for a given crystal direction the value of the limiting energy gap $\Delta(\mathbf{q},T)_{T=0}$ can assume a value different from the BCS value of $1.76k_BT_{co}$, where T_{co} is the transition temperature for the pure superconductor. In general $\Delta(\mathbf{q},T)$ depends on the direction of $\mathbf{q}$ and in some circumstances can depend on the magnitude of $\mathbf{q}$ through the selectivity of the sound wave. The $\Delta(\mathbf{q},0)$ for a given crystallographic direction is obtained by measuring the slope of a plot of $\ln(\alpha_s/\alpha_n)$ versus T_c/T over the low-temperature range, for which $f(\Delta)\sim e^{-\Delta/k_BT}$, and $\Delta(\mathbf{q},T)\sim\Delta(\mathbf{q},0)$. The measurements on pure Sn[2] indicate an anisotropy of $\sim 20\%$ for compressional-wave propagation along the [001] and [110] directions.

In addition to the dependence of the magnitude of the total electronic attenuation on ql_e, the selectivity of the electron-lattice interaction is also determined by ql_e. For example, in the limit $ql_e\gg 1$ the electron-lattice interaction becomes an electron-phonon scattering and can be treated as a simple quantum-mechanical particle-particle scattering problem. The conservation of energy and momentum requires that only electrons having a velocity component $V_F\cos\theta$ approximately equal to the sound velocity C_s, in the direction of $\mathbf{q}$, where θ is $\angle(\mathbf{V}_F,\mathbf{q})$. These electrons lie in a band near the equator of the Fermi surface. In the limit $ql_e\ll 1$, however, the interaction is best described in terms of a relaxation of all of the electrons to a Fermi surface deformed by the local ultrasonic strain field. For intermediate values of ql_e, Leibowitz[3] discussed the selectivity in terms of the angle $\theta=\Theta$ for which the amplitude of the perturbation of the electron distribution due to the sound field is reduced to half-maximum. The condition is that

$$\cos\Theta=(C_s/V_F)(+1/ql_e), \tag{3}$$

so that the interaction is weighted toward the electrons near the equator for $ql_e\gtrsim 1$. In the limit $ql_e\to\infty$, $\cos\Theta=C_s/V_F\sim 10^{-3}$. For a simple anisotropic superconductor one would therefore expect the measured $\Delta(\mathbf{q},0)$ to be a function of ql_e. However, Thomas[9] has recently demonstrated that, for Sn single crystals with fixed l_e, there is little or no change in $\Delta(\mathbf{q},0)$ for a wide range of frequencies satisfying the condition $ql_e\gtrsim 1$. This surprising result will be discussed in Sec. III.

Pokrofskii[10] has extended the calculation of ultrasonic attenuation to the case of a simple anisotropic superconductor. The temperature range of interest experimentally is that for which $k_BT_c\gg k_BT\gg\Delta(m^*C_s/\hbar k_F)^{2/3}$. In this range, the calculation yields

$$\alpha_s=A(\mathbf{q})\sqrt{(T/T_c)}\exp[-\Delta^{(n)}/k_BT], \tag{4}$$

where $\Delta^{(n)}$ is the minimum value of the energy gap on the line about the Fermi surface defined by the electron-phonon interaction, and $A(\mathbf{q})$ is related to the normal electronic attenuation. Qualitatively, this result seems correct since the low-temperature limit of a linear combination of functions such as Eq. (2) would be dominated by the lowest energy gap. The results of using Eq. (4) to fit the experimental data for Sn are discussed in Sec. III.

Tunneling data[5] indicate that in addition to a possible anisotropy associated with one piece of Fermi surface, there are several gaps observed which can be related to the multiple energy surfaces found in the higher Brillouin zones for some crystal directions in Sn. That there are multiple energy gaps in a real metal such as Sn is not surprising and in fact had been predicted previously by an extension of the BCS theory to a multiband model.[11] At present there is no detailed theory for the effect of multiple gaps on the ultrasonic attenuation. It is not at all clear what the effect of interband pairing and scattering will be on the quasiparticle-phonon scattering matrix. The simplest assumption is that of a complete neglect of interband effects, i.e.,

$$\frac{\alpha_s}{\alpha_n}=\sum_i\frac{A_i}{\exp[\Delta_i(T)/kT]+1} \tag{5}$$

where the summation is over all bands and the constants A_i are subject to the condition $\sum_i A_i=2$. This form has been used for a two-energy-gap fit for Sn with some success.[12] However, even the problem of the normal-state attenuation in a multiband metal is extremely complicated.

Pippard[13] has developed a formalism to treat the electronic attenuation in a real metal and has extended this treatment to a simple two-band model. The analysis is based on a deformation parameter which describes the alteration of the Fermi surface due to a strain field and on an inclusion of "intra-" and "inter-" band transition effects. In the limit $ql_e\ll 1$, the model predicts that the attenuation is a sum of two terms, a contribution due to intraband relaxation, as in the case of a single band, and a contribution due to interband relaxation, which results in a new equilibrium in which the number of electrons in each band is different from that for the unstrained metal. For the limit $ql_e\gg 1$, however, the attenuation is independent of the details of the relaxation process and is a sum of the contribu-

[8] T. Tsuneto, Phys. Rev. **121**, 402 (1961).
[9] R. L. Thomas, Ph.D. thesis, Brown University, 1965 (unpublished).
[10] V. L. Pokrovskii, Zh. Eksperim. i Teor. Fiz. **40**, 898 (1961) [English transl.: Soviet Phys.—JETP **13**, 628 (1961)].
[11] H. Suhl, B. T. Matthias, and L. R. Walker, Phys. Rev. Letters **3**, 552 (1959).
[12] R. W. Morse, IBM J. Res. Develop. **6**, 58 (1962).
[13] A. B. Pippard, Proc. Roy. Soc. (London) **A257**, 165 (1960).

tions of each band. Thus, if $ql_e \gg 1$, and if interband coupling can be neglected for the superconducting electrons, then Eq. (5) is a reasonable approximation. However, if interband coupling can be neglected, Suhl and Matthias[11] have shown that for a two-band superconductor there will be two transition temperatures as well as two energy gaps. On the contrary, tunneling data[5] indicate that for Sn all of the energy gaps have the BCS temperature dependence normalized to a single transition temperature T_{co}.

It is well established that small amounts of impurity added to a pure superconductor tend to reduce the transition temperature.[14] The reduction is approximately linear in l_e^{-1}, and according to the current theories[15,16] of dirty superconductivity, the decrease in transition temperature is simultaneous with a smearing out of the energy-gap anisotropy. The energy gap should be approximately isotropic when $\Delta(0) < \hbar\tau^{-1}$. For larger concentrations, the relative charge and size of the impurity ions result in different effects on the concentration dependence of both the energy gap and transition temperature.[17–19] Measurements of infrared absorption[20] and specific heat[21] indicate that the energy-gap anisotropy is reduced by doping. These properties, however, result from an average over the energy-gap spectrum, thus the measurements yield no information about the variation of the anisotropy about the Fermi surface. Although the detailed theory of the dependence of the transition temperature on impurity concentration is not reviewed here, results of measurements of transition temperature as a function of resistivity ratio for the single-crystal samples are presented in Sec. III.

II. EXPERIMENTAL TECHNIQUE

Measurements of the temperature dependence of the ultrasonic attenuation were made using the arrangement shown in Fig. 1. The pulse generator and superheterodyne receiver are contained in an attenuation comparator (Sperry). The amplitude of a pulse echo was converted to a dc signal by means of a display scanner (Hewlett-Packard 175A oscilloscope and 178A plug-in). To reduce the noise level and to eliminate dc drift, the transmitter signal was chopped and the ac signal corresponding to the amplitude of the pulse echo was detected with a lock-in amplifier (PAR JB–5). The chopping was accomplished using an external trigger source (Hewlett-Packard 412) with a binary counter to drive the ultrasonic generator n times "on" and n times "off." The number n was chosen to be sufficiently large

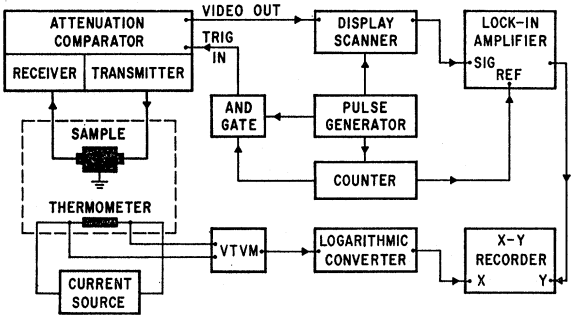

FIG. 1. Block diagram of the apparatus used to measure the temperature dependence of the ultrasonic attenuation.

to allow the display scanner to achieve the limiting voltage in each mode. A four-stage binary counter yielded $n=8$, which was sufficient for this application. In addition, the logic circuit was used to develop the square-wave reference signal for the lock-in amplifier. A three-second constant for the output filter resulted in a signal for the recorder which typically displays a noise level of less than 0.05 dB at the working level for the measurements. Matched 50-Ω lines and attenuation pads were used to reduce the standing-wave ratio. Calibration of attenuation was performed by inserting attenuation before the receiver and by always working within a 1 to 3-dB interval for variation in receiver input level to avoid nonlinearities in the receiver characteristics.

A constant current of 2 μA through a 1000-Ω carbon resistor (Speer) was used to develop a voltage which varied with temperature. The voltage was amplified by a vacuum-tube voltmeter (VTVM) (Hewlett-Packard 425); the logarithm of the signal was taken by means of a logarithmic converter (Moseley 60D) to give an output which varied approximately as T^{-1}; this output was used to drive the x axis of an x-y recorder (Moseley 2D). The resistance thermometer was calibrated at ~50-m°K intervals against the vapor pressure of the liquid helium as measured with a Bourdon-tube pressure gauge (Texas Instruments Fused Quartz Precision Pressure Gauge).

The single-crystal ingots were prepared by the Czochralski technique. The average size of the cylindrical ingots was ~8 cm long by ~3 cm diam. Ultrasonic samples were spark-cut (Servomet SMD) from the ingots into cylinders of length ~1 cm and diameter ~1 cm. The impurity-concentration gradients for the large ingots were in general less than 10%, while in the individual samples the concentration gradients were considerably less than that of the entire ingot. Impurity concentrations were determined by wet analytic chemistry and by emission spectroscopy. Resistivity measurements were made using a dc linear four-point probe technique. Tungsten probes were used for the contacts and the voltage was measured with a millimicrovoltmeter (Keithley 149).

[14] E. A. Lynton, B. Serin, and M. Zucker, J. Phys. Chem. Solids 3, 165 (1957).
[15] P. W. Anderson, J. Phys. Chem. Solids 11, 26 (1959).
[16] T. Tsuneto, Progr. Theoret. Phys. (Kyoto) 28, 857 (1962).
[17] D. Markowitz and L. R. Kadanoff, Phys. Rev. 131, 563 (1963).
[18] L. T. Claiborne, J. Phys. Chem. Solids 24, 1363 (1963).
[19] R. I. Gayley, Phys. Letters 13, 278 (1964).
[20] P. L. Richards, Phys. Rev. Letters 7, 412 (1961).
[21] R. Geiser and B. B. Goodman, Phys. Letters 5, 30 (1963).

III. EXPERIMENTAL ANISOTROPY

With the improved experimental techniques described above, a systematic comparison of the measured compressional-wave attenuation in a superconductor and the theory outlined in Sec. I was undertaken. In this section attenuation data for pure and doped Sn are analyzed in terms of Eqs. (1)–(5). The analysis has been done using a convenient nonlinear least-squares fitting technique which has general applicability.[22] The BCS temperature dependence for the energy gap has been assumed to be valid for all gaps measured in the ultrasonic experiments. This assumption has been verified by the tunneling data for Sn.[5] An analytic representation of the BCS function was employed to facilitate the data reduction, i.e.,

$$\frac{\Delta(t)}{\Delta(0)}=(1-t)^{1/2}-\frac{t(t-1)[at^3+bt^2-ct-d]}{[t-e]}, \quad (6)$$

where $a=0.40263389$, $b=0.09089008$, $c=0.12215740$, $d=0.52081285$, $e=1.0135197$. This approximation has a standard deviation of $|\delta|<3\times10^{-3}$ over most of the temperature range from the tabulated values of Muhlschlegel.[23] Near the transition temperature this approximation breaks down, and the BCS limiting expression [Eq. (9)] must be used.

First, the temperature dependence of the compressional-wave attenuation in pure Sn with $\mathbf{q}\|[001]$, [110], and [100] was analyzed assuming Eq. (2) is valid as $T\to0$. This is equivalent to the assumption underlying use of the traditional technique outlined in Sec. I. The resulting limiting energy gaps are compared in Table I with energy gaps measured by Morse *et al.*[2] The results are in good agreement with the values previously reported. Little or no change in limiting energy gap was observed as a function of frequency in agreement with the data of Thomas.[9] A possible explanation for the insensitivity of the measured gap to the selectivity of the sound wave [Eq. (3)] can be found by studying the tunneling data.[5] Zavaritskii has shown that distinct energy gaps can be identified with various regions of **k** space, hence, with various pieces of Fermi surface, consistent with the reduced-zone scheme.[24] The gaps associated with a specific region of **k** space were found to be nearly isotropic, but the gaps exhibit widely different values on going from one piece of surface to another. As discussed in Sec. I, the intersections of the planes perpendicular to **q** with the extrema of the pieces of Fermi surface according to the condition $V_F\cos\theta=C_s$ determine the group of electrons which dominates the lattice-electron interaction for $ql_e>1$. Thus, the temperature dependence of the attenuation due to the effect of the various energy gaps and deformation potentials is determined primarily by the direction of **q**. If the gap surfaces are nearly isotropic, little dependence of the measured $\Delta(0)$ on selectivity is expected for $ql_e>1$.

Analysis of the ultrasonic data on the basis of Eq. (5) for all temperatures was found to result in an extremely good fit for the temperature dependence of the attenuation; however, the indicated energy gaps were found to differ widely from the values expected on the basis of the tunneling data. For example, it is expected that two gaps [$1.5k_BT_{co}$ and $1.9k_BT_{co}$] will dominate the contribution to processes involving electrons in the [001] plane. Using Eq. (5) and assuming a two-gap fit for the pure-Sn data, with $\mathbf{q}\|[001]$, a fit within the experimental error is obtained over the entire temperature range for $A_1\sim1.5$, $\Delta_1(0)\sim1.4k_BT_{co}$, and $\Delta_2(0)\sim4k_BT_{co}$. Since the lower gap dominates over most of the temperature range, the determination of $\Delta_1(0)$ is much better than that of $\Delta_2(0)$. An energy gap as low as $1.4k_BT_c$ has been measured by tunneling methods[5]; however, $\Delta_2(0)$ appears to be much too large to be physically meaningful. For the plane perpendicular to the [110] direction a two-gap fit to the data seems impractical since tunneling data indicate that at least four gaps will contribute. Even for this case, Eq. (5) leads to a reasonable approximation for the temperature dependence of the attenuation. The values of the constants in Eq. (5) for several In-doped Sn samples are presented in Table II. These values are of interest since a combination of Eqs. (5) and (6) leads to a good representation of the ultrasonic data for future theoretical comparisons.

The ultrasonic data have also been analyzed on the basis of Eq. (4). If the term $\sqrt{(T/T_c)}$ is dropped, Eq. (4) is similar to the low-temperature limit of Eq. (2). Some representative values of $\Delta^{(n)}$ and A, where A

TABLE I. Comparison of pure-Sn energy-gap [$2\Delta(0)$] measurements.

q	Current work [k_BT_{co}]	Morse *et al.*[a] [k_BT_{co}]
$\|$ [001]	(3.26±0.02)	(3.2±0.1)
$\|$ [110]	(3.94±0.04)	(3.8±0.1)
$\|$ [100]	(3.62±0.04)	(3.5±0.1)

[a] Reference 2.

TABLE II. Two-gap fit for In-doped Sn.

	ρ	Δ_1/k_BT_{co}	Δ_2/k_BT_{co}	A_1
[001]	0	1.43	4.32	1.56
	0.0020	1.49	6.22	1.71
	0.0035	1.58	4.58	1.71
	0.0093	1.78	···	2.00
[110]	0	1.68	4.89	1.41
	0.0020	1.83	7.66	1.86
	0.0065	1.73	8.42	1.94
	0.0091	1.73	···	2.00

[22] D. W. Marquardt, SHARE General Program Library, DPE NLIN (PA) 3094, 1964 (unpublished).
[23] B. Muhlschlegel, Z. Physik **155**, 313 (1959).
[24] T. Olsen, in *The Fermi Surface*, edited by W. A. Harrison and M. B. Webb (John Wiley and Sons, Inc., New York, 1960), p. 237.

$=A(\mathbf{q})/\alpha_n$, are given in Table III as computed both with and without the term $\sqrt{(T/T_c)}$. It is interesting to note that when A is treated as a variable, the best fit is obtained for $A\sim1$ rather than $A\sim2$, as in the low-temperature limit of Eq. (2). Physically, this result should indicate the relative contribution of the low-energy-gap electrons to the total attenuation. However, the indicated energy gaps are somewhat lower than those given by the tunneling data, and the physical significance of the constants in Table III is open to question.

The present theory of impure superconductors[15] (cf. Sec. I) predicts that the reduction in relaxation time due to impurity scattering causes a reduction in energy-gap anisotropy. The effect of anisotropy on the transition temperature has been studied theoretically[16,17] and experimentally.[14] It has been shown[25] that the limiting energy gap obtained from ultrasonic attenuation measurements depends on impurity concentration and can be used to determine the relative anisotropy in doped Sn single crystals. The limiting energy gaps for $\mathbf{q}\|[001]$, [110], and [100] have been measured in a variety of In-, Cd-, Bi-, and Sb-doped single crystals and compared on the basis of transition temperature and resistivity ratios.

The measured changes in transition temperature (ΔT_c), for the samples used in these experiments, are plotted as a function of resistivity ratio in Fig. 2. Also included are some ΔT_c values for polycrystalline samples as reported in Ref. 14 (designated LSZ) as well as some theoretical curves (designated MK) from Ref. 17. The lowest theoretical curve is obtained by considering the effect of the electron mean free path alone. The upper two curves include the "valence" effect for Sb and Cd, respectively, as given in Ref. 16. The magnetically corrected value of the transition temperature in pure Sn was measured to be 3.7254°K, in good agreement with the value listed in Ref. 14. It is found that the ΔT_c values for the single-crystal samples are in rough agreement with the polycrystalline data. There is sufficient scatter in both cases to prohibit a detailed investigation of the effects of the valence and size mismatch between the solute and solvent ions. This scatter for the single-crystal samples reflects the poor accuracy of the resistivity-ratio measurements.

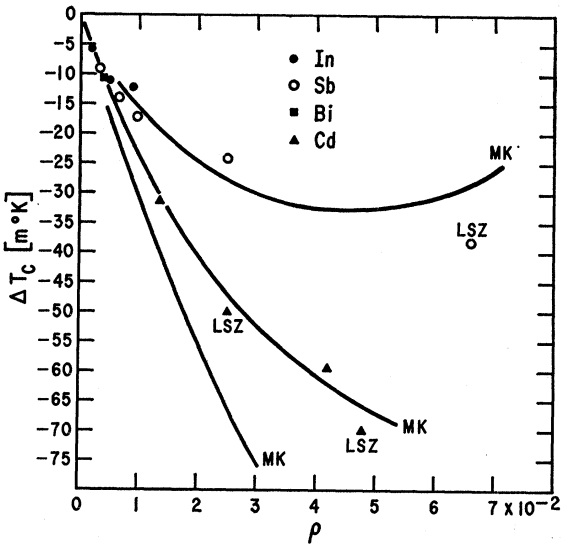

FIG. 2. The change in transition temperature (ΔT_c) from that of pure Sn as a function of inverse resistivity ratio for several impurities. The theoretical curves (Ref. 17) for Sb- and Cd-doped Sn are labeled MK. Some polycrystalline data points (Ref. 14) are labeled LSZ.

In Fig. 3, the energy gaps, in units of k_BT_{co}, are plotted as a function of $(-\Delta T_c)$. The curves in Fig. 3 show the limiting energy gaps for $\mathbf{q}\|[110]$, $\mathbf{q}\|[100]$, and $\mathbf{q}\|[001]$, respectively, as determined by an analytic fit of data from $\sim$1.2 to 2.2°K assuming the single-gap BCS model. The reduction in anisotropy is obvious, and the value of $\Delta(0)$ toward which the gaps tend lies between 1.75 and 1.80, consistent with the BCS prediction of 1.76 and in agreement with the infrared-absorption[20] and specific-heat[21] data. Although it has been shown that the selectivity of the sound wave does not greatly affect the value of the limiting energy gap, a precaution was taken to minimize the possibility of such an effect in the more heavily doped samples; this was accomplished by increasing the measurement frequency in direct proportion to the change in resistivity ratio. Measurements were made over the frequency

TABLE III. Constants for fit to Pokrovskii's limiting formula.

q	With $\sqrt{(T/T_c)}$ A	With $\sqrt{(T/T_c)}$ $\Delta^{(n)}/k_BT_{co}$	Without $\sqrt{(T/T_c)}$ A	Without $\sqrt{(T/T_c)}$ $\Delta^{(n)}/k_BT_{co}$
Pure Sn				
[110]	1.027	1.347	1.150	1.596
[001]	0.919	0.942	1.034	1.200
0.01% In				
[110]	1.069	1.294	1.196	1.542

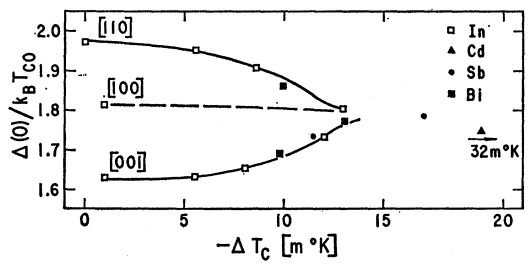

FIG. 3. The limiting energy gaps in units of k_BT_c for a "one-gap" extrapolation with (a) $\mathbf{q}\|[110]$, (b) $\mathbf{q}\|[100]$, and (c) $\mathbf{q}\|[001]$ in In-, Cd-, Sb-, and Bi-doped Sn single crystals plotted as a function of the change in transition temperature measured for each sample.

[25] L. T. Claiborne and N. G. Einspruch, Phys. Rev. Letters 15, 862 (1965).

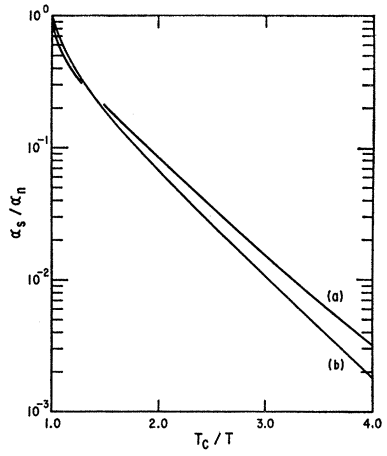

FIG. 4. $\ln(\alpha_s/\alpha_n)$ versus T_c/T for $\mathbf{q}\|[001]$ in (a) pure Sn and (b) 0.1 at. % In-doped Sn. Note: The impurity concentrations referred to here and throughout the text are nominal values for the ingots from which the samples were prepared.

range from 50 MHz for pure Sn to 460 MHz for the more heavily doped samples. The total electronic attenuation ranged from 28 dB cm^{-1} to 15 dB cm^{-1}, indicating that the ql_e variation was at worst less than a factor of 2.

Figure 4 is a plot of $\ln(\alpha_s/\alpha_n)$ versus T_c/T for $\mathbf{q}\|[001]$ in (a) pure Sn, and (b) $\sim$0.1 at.% In-doped Sn, for which $\Delta T_c \sim -15m$°K. The change in energy gap is obvious, and the data for (b) fit the BCS function over the entire temperature range within a standard error of $\sim$0.4% of the total electronic attenuation, which is approximately the observed experimental error. This result is an additional verification of the validity of the BCS theory for an isotropic superconductor.

In Fig. 5 the limiting energy gap is plotted as a function of resistivity ratio for a number of doped samples with $\mathbf{q}\|[110]$ and [001] directions. Again, the reduction in anisotropy is evidently a smooth function of average electron relaxation time. It is clear that the anisotropy of the limiting energy gap of Sn is greatly reduced for $|\Delta T_c| > 15$m°K or for $\rho > 10^{-2}$. Using the data included in Ref. 17, one can estimate the resistivity ratio for which $\tau \sim \hbar/\Delta(0)$ and for which one expects the reduction in anisotropy to become important for Sn, i.e., $\tau \sim \hbar/\Delta(0)$ implies that $\rho \sim 1.1 \times 10^{-2}$. The results

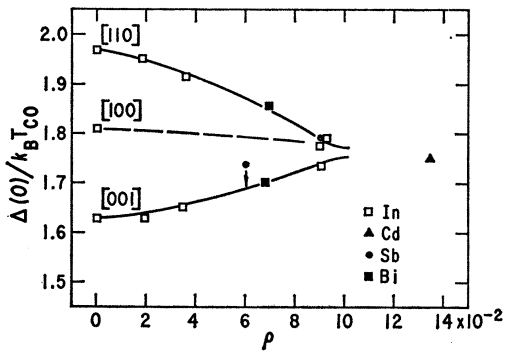

FIG. 5. The limiting energy gaps as in Fig. 4 plotted as a function of the measured inverse resistivity ratio.

are in quite good agreement with the theoretical prediction.

It must be emphasized that the limiting energy gap is related to the smaller energy gaps of Sn. One expects the relaxation times associated with interband and intraband processes to be affected differently by the impurity concentration. It is therefore of interest to ascertain if the ultrasonic data contain any additional information which can be related to the larger energy gaps. Some qualitative results are discussed in Sec. IV.

IV. THE EFFECTIVE ENERGY GAP

In the previous section the attenuation data were analyzed in terms of existing models. In this section the data are studied from a strictly experimental viewpoint. Although some interesting observations can be made, any conclusions reached in this section should be taken as tentative pending a more complete theoretical model for the multigap superconductor.

The availability of the tunneling data permits a more detailed examination of the meaning of the effective energy gap observed in ultrasonic measurements. Consider the effective gap defined by

$$\Delta_{\text{eff}}(\mathbf{q},T) \equiv k_B T \ln[2/\alpha(T) - 1], \tag{7}$$

where $\alpha(T) \equiv \alpha_s(T)/\alpha_n$. This definition is equivalent to setting the right-hand side of Eq. (2) equal to the correct attenuation function $G(\Delta_1,\Delta_2,\cdots,A_1,A_2,\cdots,T)$, where $\{\Delta_i\}$ are the contributing energy gaps and $\{A_i\}$ are the appropriate weighting factors. In order to emphasize the difference between the effective gaps for the anisotropic and isotropic cases, Eq. (7) was normalized to the isotropic gap at all temperatures. Since the isotropic limiting gap was shown to be approximately equal to the BCS value and Eq. (2) was found to hold for the heavily doped superconductors, the normalization can be written as

$$\frac{\Delta_{\text{eff}}(T)}{\Delta_{\text{BCS}}(T)} = \frac{T}{1.76 T_c F(T)} \ln\left[\frac{2}{\alpha(T)} - 1\right], \tag{8}$$

where $F(T)$ is approximated by Eq. (6).

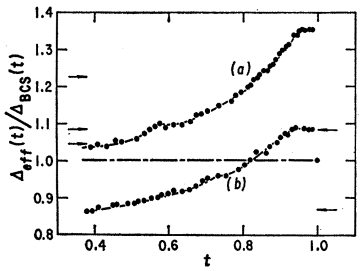

FIG. 6. The normalized energy gap at 50MHz as defined by Eq. (7) for (a) $\mathbf{q}\|[110]$ and (b) $\mathbf{q}\|[001]$ in pure Sn plotted as a function of reduced temperature. The normalized energy gaps, obtained from tunneling data, which contribute are indicated by arrows on the left for $\mathbf{q}\|[110]$ and on the right for $\mathbf{q}\|[001]$.

Figure 6 is a plot of the temperature dependence of the normalized effective gap for $\mathbf{q}\|[110]$ and [001] in pure Sn. Tunneling data reveal that there should be major contributions to the attenuation function G from only two gaps for $\mathbf{q}\|[001]$ directions, i.e., $1.55k_BT_{co}$ and $1.9k_BT_{co}$. The normalized values of these gaps are indicated by arrows at the right-hand side of Fig. 6. Near T_{co} the effective gap is approximately equal to the upper gap from tunneling data, and near $T=0$ the effective gap is approximately equal to the lower gap. Several gaps contribute to the $\mathbf{q}\|[110]$ direction, as indicated by arrows on the left-hand side of Fig. 6. For this case the effective gap near T_{co} is somewhat larger than the upper gap from the tunneling data, but the effective gap near $T=0$ appears to be in good agreement with the lowest gap value. The limiting gaps from ultrasonic data for $\mathbf{q}\|[001]$, [110], and [100] are compared with the tunneling data in Table IV. The relative weight of the contribution of each gap to the ultrasonic attenuation is estimated from the tunneling data. The agreement between the results of the two

TABLE IV. Comparison of the energy-gap values (in units of k_BT_{co}) from tunneling data and from the normalized effective energy-gap plots for the ultrasonic data.

	Weight	Tunneling	Ultrasonic	Limit
[001]	Large	1.8–1.9	1.92	$t\to 1$
	Large	1.55	1.51	$t\to 0$
[110]	Large	2.2	2.38	$t\to 1$
	Medium	1.8–1.9	1.92	$t\to 0$
	Small	1.7	?	
		1.5		
[100]	Large	2.2	2.20	$t\to 1$
	Medium	1.8–1.9	?	
	Medium	1.78	1.81	$t\to 0$
	Small	1.55	?	

methods is remarkably good considering that there is, as yet, no theoretical model to justify this identification.

Near T_{co} the ratio of the effective energy gap to the BCS gap approaches a constant. It is instructive to compare the temperature dependence of the effective gap to the predictions of the BCS theory near T_{co}, i.e.

$$\Delta(T)\cong 1.74\Delta(0)[1-t]^{1/2}. \tag{9}$$

Figure 7 is a plot of $\log\Delta_{\text{eff}}(T)$ versus $\log[1-t]$ for $\mathbf{q}\|[110]$ and [001]. Lines of slope $\frac{1}{2}$ have been drawn through each set of data near T_c. The fit is quite good. Furthermore, if one assumes that the constant (1.74) is correct in Eq. (9), the $\Delta(0)$ for $\mathbf{q}\|[001]$ is $1.92k_BT_c$ and for $\mathbf{q}\|[110]$ is $2.38k_BT_c$, compared to the tunneling values of $1.9k_BT_c$ and $2.2k_BT_c$, respectively. If the behavior of the attenuation near T_c is truly single-gap-like, then compressional-wave ultrasonic-attenuation studies should provide the most sensitive tool for measuring the gap as a function of temperature because of the large changes in attenuation which occur near T_c.

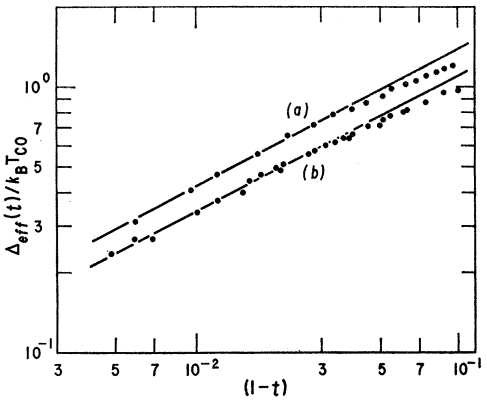

FIG. 7. The effective energy gap at 50 MHz for (a) $\mathbf{q}\|[110]$ and (b) $\mathbf{q}\|[001]$ plotted as a function of $(1-t)$. The solid lines indicate slopes of $\frac{1}{2}$.

The problem of relating the traditional limiting energy gap at absolute zero from ultrasonic-attenuation studies to the actual energy gaps which are contributing to the temperature dependence of the attenuation is considered now. It should be noted that the effective energy gaps at low temperatures in Fig. 6 are only becoming BCS-like as the temperature is lowered, but that there is still a small contribution from the larger energy gaps. Thus, an analytic, single-gap fit, such as described in Sec. III, will tend to average in some contribution from the larger gaps and overestimate slightly the lowest energy gap. It should also be noted there has always been a problem in extrapolating the ultrasonic-attenuation data to the absolute-zero value, α_0. The theoretically significant ratio of superconducting to normal attenuation $\alpha(T)$ is $[\alpha_s(T)-\alpha_0]/(\alpha_n-\alpha_0)$. At low temperatures $\alpha_s(T)$ is very close to α_0; hence, small errors in α_0 introduce large errors in the effective energy gap. For the traditional graphical method illustrated in Fig. 4, α_0 is adjusted until a plot of $\ln\alpha(T)$ versus T_c/T gives the best straight-line fit at low temperatures. For the analytic method of Sec. III, α_0 is left as a variable parameter for the least-squares fitting. Both the single-gap and two-gap methods of Sec. III give approximately the same value of α_0 for $\mathbf{q}\|[001]$ and [110] directions; therefore, these values are used with some confidence. However, the situation is much more complicated for $\mathbf{q}\|[100]$, as is illustrated in Fig. 8. Independent of what value of α_0 is chosen, there is always a kink in the normalized effective-gap curve near a reduced temperature of 0.55. Thus, if the single-gap analytic method is used the value of the limiting energy gap and α_0 depend strongly on the initial temperature chosen for the fit. Table V demonstrates the change in parameters for three initial temperatures. The relative α_n for these data is $+2.92$ dB cm^{-1}.

Curves (a) and (b) of Fig. 8 correspond to the first two fits, respectively, described in Table V. Curve (c) is the result of assuming the two-gap extrapolation for

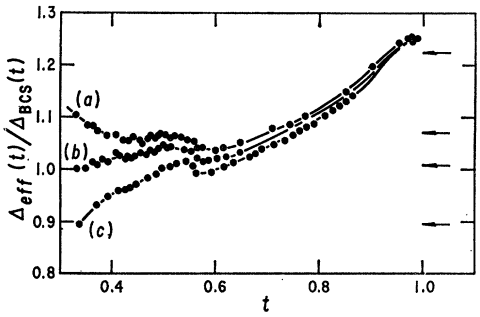

FIG. 8. The normalized effective energy gap for $\mathbf{q}\|[100]$ in pure Sn at 50 MHz plotted as a function of reduced temperature for different values of α_0: (a) $\alpha_0=-24.118$ dB cm^{-1}, (b) $\alpha_0=-24.214$ dB cm^{-1}, and (c) $\alpha_0=-24.447$ dB cm^{-1}.

α_0 to be correct, i.e., $\alpha_0=-24.447$ dB cm^{-1}. Curve (b) would obtain for the traditional graphical fit. One reasonable explanation for the complications when $\mathbf{q}\|[100]$ can be found from a consideration of the gaps which contribute. There should be a rather large contribution from a gap at $1.8k_BT_c$ and a somewhat smaller contribution at $1.6k_BT_c$. Curve (c) of Fig. 8 is consistent with the onset of a Pokrovskii region for the lowest gap which begins for $t<0.5$ while in the neighborhood of $t=0.5$ the $1.8k_BT_c$ gap appears to dominate. However, there may be other explanations to be found when the correct G is determined for Sn.

The validity of the quantitative comparisons which have been made in the preceding few paragraphs is admittedly open to question. However, since the normalized effective gap reflects the various contributing energy gaps for pure Sn, the temperature variation of the effective gap for the alloys should reflect the reduction in anisotropy of all the gaps and provide a qualitative tool for studies of the doped Sn. Figure 9 is a plot of the normalized effective energy gap for (a) pure Sn, (b) Sn+0.05% In, and (c) Sn+0.1% In, with $\mathbf{q}\|[001]$. Note that for curve (b) the upper gap contribution is little affected by the impurity content, but that a change in the limiting gap for small t is observed. In curve (c) all of the anisotropy for this direction is

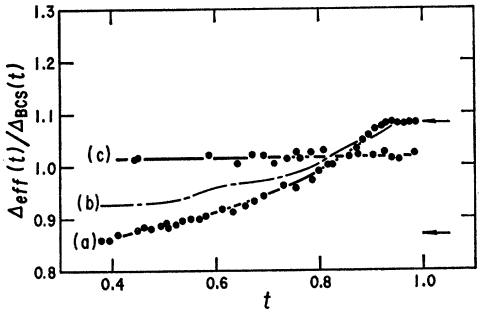

FIG. 9. The normalized effective energy gap for $\mathbf{q}\|[001]$ in (a) pure Sn, (b) Sn+0.05% In, and (c) Sn+0.1% In plotted as a function of reduced temperature. The arrows on the right indicate the normalized energy gaps for this direction as determined by tunneling measurements.

TABLE V. The effects of the initial temperature on the constants obtained for a one-gap fit to the data for $\mathbf{q}\|[100]$.

Initial temperature (°K)	α_0 (dB cm^{-1})	$\Delta(0)$ (k_BT_{co})	$\Delta_{eff}(0)/\epsilon(0)$
1.941	−24.118	1.866	1.060
2.301	−24.214	1.817	1.032
2.642	−24.097	1.863	1.059

apparently removed. Figure 10 shows the normalized effective energy gap with $\mathbf{q}\|[110]$ for (a) pure Sn, (b) Sn+0.01% In, and (c) Sn+0.05% In. Note that in curve (b) the small impurity concentration affects the largest gap contribution much more drastically than the lowest gap contribution.

Figures 9 and 10 provide evidence of the complicated manner in which the gap anisotropy is removed. As was pointed out in Sec. III, the single relaxation-time approximation of Markowitz and Kadanoff[17] is not adequate to describe the anisotropy removal for a multigap superconductor. For example, ionized-impurity scattering results in different relaxation times for the intraband as well as for the interband relaxation. In the limit of the Born approximation for parabolic bands, it can be shown that the intraband relaxation time goes as $\tau\propto V_F^3$, where V_F is measured from the bottom of the band. Thus, it is expected that to a first approximation the anisotropy of the small pieces of Fermi surface will be removed at lower concentrations than required for larger pieces and that interband anisotropy will remain at even higher concentrations. It is then tempting to apply this interpretation to Figs. 9 and 10. The changes between the effective-gap curves (a) and (b) would be predominantly associated with intraband effects, while the changes between curves (b) and (c) would be predominantly associated with interband effects. This identification is at least consistent with Zavaritskii's interpretation of the tunneling data.

Finally, the ultrasonic data indicate that the gaps observed near T_{co} for $\mathbf{q}\|[100]$ and [110] are associated with the surface for which Zavaritskii found a single

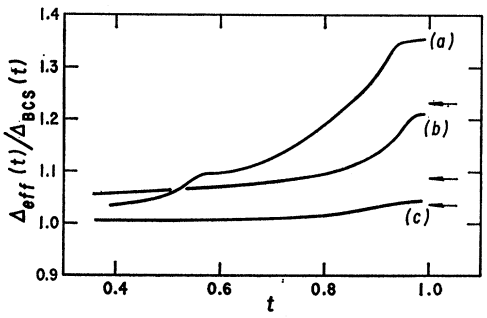

FIG. 10. The normalized effective energy gap for $\mathbf{q}\|[110]$ in (a) pure Sn, (b) Sn+0.01% In, and (c) Sn+0.05% In plotted at a function reduced temperature.

isotropic gap. Also, the anisotropy of this gap appears to be removed by the addition of a very small amount of impurity ($\sim$0.01% In) as measured by the ultrasonic technique. Tunneling studies applied to pieces of Fermi surface located away from the center of the Brillouin zone are hampered by the fact that the **k** vector relevant to the appropriate density of states for the tunneling current is measured from the zone center. Thus, it is difficult or impossible to obtain by tunneling the energy gap for a direction perpendicular to the axis of such a surface. For this very special case the ultrasonic technique should supply more information about the energy-gap anisotropy than the tunneling technique.

V. CONCLUSIONS

The research reported above has led to several definite conclusions and has also provided a motivation for further ultrasonic studies in pure and doped superconductors. Two definite needs for future research in this area have been illustrated: (1) the need for a more complete theory for compressional-wave attenuation in a multigap superconductor, and (2) the need for detailed tunneling studies in single crystals of doped Sn to complement the ultrasonic data. The conclusions reached are as follows:

(1) There is a distinct reduction in the anisotropy of doped Sn as indicated by the limiting energy gap determined from the temperature dependence of the compressional-wave ultrasonic attenuation for $|\Delta T_c|>15$ m°K and for $\rho>10^{-2}$.

(2) The temperature dependence of the superconducting energy gap near T_c predicted by the BCS theory has been confirmed.

(3) Information about the larger energy gaps for Sn is contained in the temperature dependence of the compressional-wave attenuation, and from a direct comparison with the tunneling data it appears that this information can be obtained in a straightforward manner.

(4) Normalized plots of the effective energy gap as defined by Eq. (8) can be used for qualitative studies of the gap anisotropy and the selectivity of the sound wave.

It has been possible to shed light on the meaning of the limiting energy gap as determined by the traditional ultrasonic measurements. Some of the problems involved in relating the limiting gap to real gaps have been pointed out. Finally, it has been demonstrated that ultrasonic-attenuation data can be used to complement tunneling data particularly in relating measured energy gaps to specific regions of **k** space.

ACKNOWLEDGMENTS

The authors thank R. T. Bate for many helpful discussions and acknowledge with thanks the contributions made to this work by G. R. Cronin, D. Thompson, R. B. Hemphill, W. R. Hardin, E. L. Jones, Mrs. M. White, and J. L. Rooke.

APPENDIX: GLOSSARY

A_i ≡Weighting constant for contribution to superconducting attenuation of ith group of electrons.
$A(\mathbf{q})$ ≡Pokrovskii weighting constant for superconducting attenuation at low temperatures.
C_s ≡Compressional wave velocity≡$\omega/|\mathbf{q}|$.
$\hbar$ ≡Planck's constant divided by 2π.
k_B ≡Boltzmann's constant.
$\mathbf{k}_F$ ≡Wave vector of electron at Fermi surface.
l_e ≡Electron mean free path.
N ≡Number of electrons per unit volume.
m_e ≡Mass of free electron.
m^* ≡Effective mass of electron.
R ≡Ratio of resistance at room temperature to that at 4.2°K.
T ≡Temperature.
T_c ≡Superconducting transition temperature.
T_{c0} ≡Superconducting transition temperature for pure Sn.
ΔT_c ≡$T_{c0}-T_c$.
t ≡T/T_c.
α_n ≡Impurity limited compressional-wave attenuation in the normal state.
$\alpha_s(T)$ ≡Compressional-wave attenuation in the superconducting state at temperature T.
α_0 ≡Extrapolated compressional-wave attenuation at absolute zero.
$\Delta(\mathbf{q},0)$ ≡Limiting energy gap at absolute zero from a fit of $\alpha_s(T)$ to Eq. (2) at low temperatures.
$\Delta_{\text{eff}}(T)$≡Effective energy gap at temperature T from compressional-wave ultrasonic attenuation and Eq. (2).
$\Delta^{(n)}$ ≡Minimum energy gap on equator of Fermi surface perpendicular to **q**.
$\epsilon_0(T)$ ≡BCS value of isotropic energy gap at temperature T.
θ ≡Angle between **q** and $\mathbf{k}_F$.
Θ ≡Angle between **q** and $\mathbf{k}_F$ at which the perturbation to the electron distribution due to sound wave becomes half-maximum.
ρ ≡R^{-1} the inverse resistivity ratio.
ρ_0 ≡Density of the crystal.
τ ≡Isotropic electron relaxation time.
ω ≡2π times the sound frequency.